Magnetic ordering in rare-earth fluorides with KY_3F_{10} structure and axial moments

Stephen L. Chamberlain* and L. R. Corruccini†
Physics Department, University of California, Davis, Davis, California 95616, USA
(Received 22 March 2004; revised manuscript received 1 November 2004; published 31 January 2005)

The rare-earth fluorides with the cubic KY_3F_{10} structure contain rare-earth sites having tetragonal symmetry, with one-third of the sites having symmetry axes aligned along each of the cubic axes. We present the magnetic properties for compounds in which Er^{3+}, Yb^{3+}, Tm^{3+}, and Tb^{3+} substitute for Y^{3+}. Similar to KDy_3F_{10}, reported earlier, these materials display nearly complete (Ising) anisotropy of the magnetic moments along the local symmetry axis, yielding three orthogonal Ising lattices. Estimates of magnetic exchange are antiferromagnetic in all compounds, and the dipole-dipole interaction favors antiferromagnetism in the absence of exchange in each case. At low temperature, we find that only the Tm compound clearly displays antiferromagnetic order, while in the Er and Yb compounds we observe a transition to a ferromagnetic state, very similar to that seen in KDy_3F_{10}. We suggest a reason for this by comparing ground state energies as a function of single-ion anisotropy and the magnitudes of the two interactions.

DOI: 10.1103/PhysRevB.71.024434 PACS number(s): 75.30.Cr, 75.50.Dd

I. INTRODUCTION

The rare-earth compounds isomorphous with KY_3F_{10} have a novel cubic structure, containing three magnetically nonequivalent sites for the rare-earth ions. The structure was first analyzed by Hong and Pierce[1] and is pictured in Fig. 1. The space group is fcc ($Fm3m$) but the symmetry of the rare earth sites is tetragonal (C_{4v}), with the fourfold symmetry axis oriented along one of the three cubic axes. The magnetic ions are separated by a minimum distance of approximately 3.9 Å. To first order, they can be pictured as occupying the approximate face centers of a simple cubic lattice with a cube edge half the value of the full structure. They are located at the vertices of a network of corner-sharing octahedra, producing a structure which is partially frustrated in the presence of antiferromagnetic exchange. In several of these compounds, containing Dy^{3+}, Er^{3+}, Yb^{3+}, Tm^{3+}, and probably Tb^{3+}, the magnetic moments of the rare earth ions are almost completely anisotropic, with a large component parallel to the local tetragonal axis and an orthogonal component too small to measure in most cases. These unique materials thus contain three identical but orthogonal Ising systems. As a consequence of the structure and the extreme anisotropy of the moments, simple single-axis magnetic order is not possible and the ordered state must necessarily be more complex.

These materials share some features with the better-known tetragonal $LiYF_4$ compounds.[2] The rare earth point symmetry is tetragonal in both cases, and the rare earth separation and density are very similar.[3] In both classes of materials, magnetic interactions are weak, and the effect of the dipole-dipole interaction is important. In most of the $LiYF_4$ materials, the ordered magnetic state is predicted correctly by the dipole-dipole interaction alone.[4,5] In addition to the very interesting structural characteristics of the title compounds, we were motivated to study their magnetic properties by a curiosity about whether their magnetic order is similarly dominated by the dipolar interaction. Because of the unusual structure of these materials, in which nearest-neighbor spins are nearly orthogonal, one might expect the effect of exchange to be drastically reduced, perhaps negligible. Instead we find, in common with certain frustrated pyrochlores, notably "spin ice,"[6] that both exchange and dipolar interactions must be taken into account to understand the KY_3F_{10} compounds. Taken separately, both exchange and dipole-dipole interactions favor antiferromagnetic order. We previously reported that KDy_3F_{10} surprisingly displays ferromagnetism at low temperature.[7] In this paper we de-

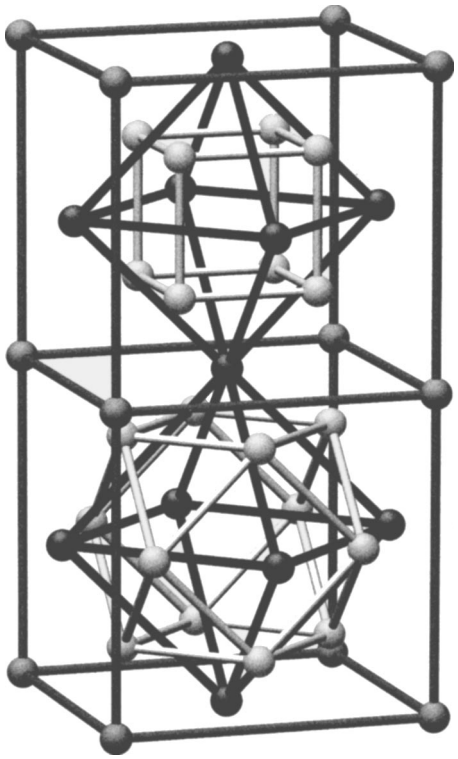

FIG. 1. The primitive fcc unit cell for the KY_3F_{10} structure. The darkest spheres represent rare earth ions, the lightest ones fluorine, and the intermediate ones potassium. The rare earth ions occupy the vertices of a network of corner-sharing octahedra; each ion has point symmetry C_{4v} about an axis oriented parallel to one of the cubic axes.

scribe the magnetic properties of KEr_3F_{10}, KYb_3F_{10}, KTm_3F_{10}, and KTb_3F_{10}, at least two of which show very similar behavior, and at least one of which orders antiferromagnetically. We suggest that the antiferromagnetic case is due to much larger single-ion anisotropy.

II. EXPERIMENTAL METHODS

Samples of KEr_3F_{10}, KYb_3F_{10}, KTm_3F_{10}, and KTb_3F_{10} were made by combining and mixing the powders of the appropriate rare earth trifluoride with KF in stoichiometric ratio. The starting materials were dried by heating in vacuum at 200 °C before combining in an argon-filled glove box. To eliminate residual oxide contamination, 10% NH_4HF_2 was added to the samples, which were then heated in a Ni boat under flowing argon at 350 °C for several hours. Transparent single crystals of KEr_3F_{10} and KTb_3F_{10} were grown from the powdered samples in sealed Ni crucibles using the Bridgman technique, at temperatures slightly over 1000 °C. KTm_3F_{10} crystallized into a noncubic phase from the melt, and KYb_3F_{10} produced only polycrystalline samples with mixed cubic and monoclinic phases using this method, so these two materials were grown in (cubic) polycrystalline form using solid state reaction at 600 °C, in a sealed, evacuated Ni crucible. Subsequent chemical analysis found no detectible Ni impurities. Powder x-ray diffraction spectra of the completed samples were very clean. All peaks could be indexed to the cubic KY_3F_{10} structure, with the exception of KTm_3F_{10} which contained a single small impurity peak about 1% of the magnitude of the largest peak. We obtain lattice constants of 11.517 Å (KEr_3F_{10}), 11.404 Å (KYb_3F_{10}), 11.454 Å (KTm_3F_{10}), and 11.681 Å (KTb_3F_{10}), all reasonably consistent with previously reported values.[8–10]

Static magnetic susceptibilities were measured using shaped spherical samples (single crystal or packed polycrystalline) with diameters of 1 to 2.5 mm. Above 1.7 K, data were obtained using a Quantum Design MPMS squid magnetometer, at fields of 10 mT, 30 mT, and 50 mT. Within experimental error, susceptibility was independent of field in this range. Below 2.5 K, samples were cooled inside the mixing chamber of a dilution refrigerator, and magnetization was measured using fluxgate magnetometers. Susceptibility measurements were taken at fields of 1, 10, and 50 mT, with the lowest field useful primarily at the lowest temperatures. Data taken with the dilution refrigerator were normalized to agree with data taken in the squid magnetometer in the range 1.7–2.5 K. Temperature was measured using a CMN thermometer at 1 mT, and with a germanium resistance thermometer, down to 70 mK only, at 10 and 50 mT. Both were located inside the mixing chamber next to the samples. Accuracy in the temperature readings is estimated to be about 2% above 30 mK, and ±0.6 mK below 30 mK.

III. EXPERIMENTAL RESULTS AND DISCUSSION

The susceptibility of KEr_3F_{10} in the temperature range below 2.0 K is shown in Fig. 2. This material does not obey a Curie-Weiss law in this region, possibly due to spin-spin interactions. A mean-field analysis of the susceptibility was carried out at temperatures above 10 K, assuming $\chi^{-1}=\chi_o^{-1}-\lambda$, shown in Fig. 3. Here χ_o is the susceptibility without interactions, calculated from spectroscopically determined crystal field parameters,[11,12] and $\lambda=-0.070\pm0.015$ mol/cm^3 is the mean field interaction constant, fitted to the data. The T intercept of the extrapolated $\chi_o^{-1}-\lambda$ vs T plot yields a value for the Weiss constant of $\theta_W=-0.71\pm0.15$ K. Within experimental error, this is the same as the mean-field expectation $\theta_W=C\lambda$, where $C=N_o\left(\frac{1}{3}g_\parallel^2+\frac{2}{3}g_\perp^2\right)\mu_B^2S(S+1)/3k_B$ is the low-temperature Curie constant, calculated from the experimental g factors of the Er^{3+} ground state. These have been measured

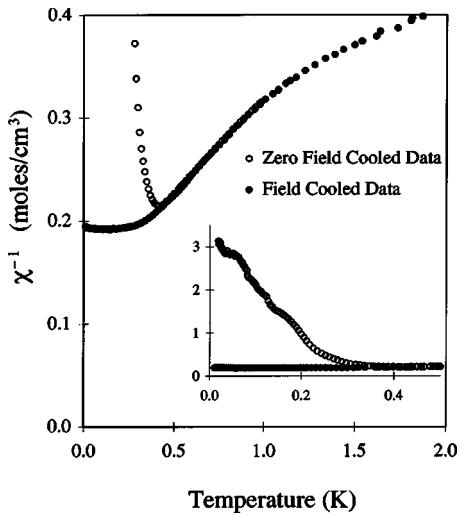

FIG. 2. Inverse susceptibility of KEr_3F_{10} below 2.0 K. Below approximately 0.3 K, the FC susceptibility data are nearly constant and equal to about 60% of the demagnetization limit, suggestive of a spontaneous magnetization. The ZFC susceptibility is much smaller below this knee, consistent with increased pinning of ferromagnetic domain walls at lower temperatures. The insert displays the full range of data below 0.2 K.

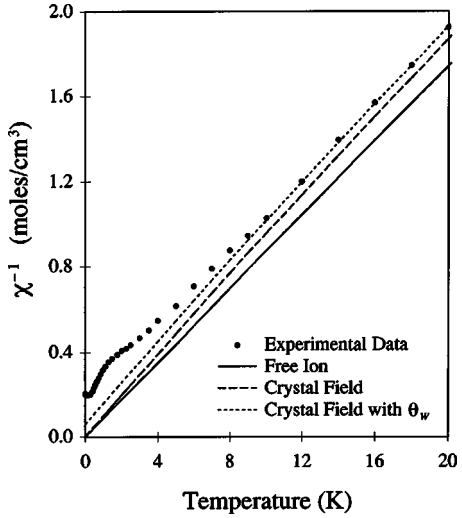

FIG. 3. Inverse susceptibility of KEr_3F_{10} from 0 to 20 K. The upper dashed line is a mean-field fit to data above 10 K, assuming $\chi^{-1}=\chi_o^{-1}-\lambda$, where χ_o is calculated from spectroscopically-determined crystal field parameters, and $\lambda=\theta_W/C$ is the fitted mean field parameter.

by Zeeman spectroscopy to be $g_{\|}=17.6$ and $g_{\perp}<0.1$.[13] There is a knee in the field cooled data in the vicinity of 0.3 K, below which the susceptibility is nearly constant at $\chi_{\max}=5.3$ cm^3/mol. The corresponding dimensionless susceptibility is $\chi_{\max}/V_{mol}=0.137$, nearly 60% of the demagnetization limit $1/N$ for a spherical sample, equal to $(4\pi/3)^{-1}=0.239$, where N is the sample demagnetization factor. This is similar to the behavior observed at low temperature in a variety of ferromagnets,[14,15] and very much like that observed earlier in the isostructural KDy_3F_{10}.[7] Zero-field-cooled susceptibilities become much smaller than field-cooled values below about 0.3 K, consistent with increased pinning of ferromagnetic domain walls at lower temperature, again very similar to the behavior of KDy_3F_{10}.

Within the mean-field approximation, for a spherical sample, θ_W is the sum of parts due to the exchange and dipole-dipole interactions:[15] $\theta_W=\theta_W^{ex}+\theta_W^{dip}$, where θ_W^{dip} is given by a lattice sum.[16] For the KY_3F_{10} materials, the expression is given by

$$\theta_w^{dip}=-\frac{\mu_B^4}{8Ck_B^2}\sum_{ij} g_{i,3}^2 g_{j,3}^2\left(\frac{1}{r_{ij}^3}-\frac{3z_{ij}^2}{r_{ij}^5}\right), \tag{1}$$

where C is the Curie constant and $g_{i,3}$ is the zz component of the g tensor for the doublet ground state of ion i. The summation over i is taken over the three independent magnetic sites in the crystal, while the summation of j is taken over successive spherical shells with a thickness of one unit cell out to a radius of 200. The general result for axially symmetric moments is

$$\theta_w^{dip}=\frac{\mu_B^2}{4Pk_Ba^3}[-g_{\perp}^4(141.00)+g_{\perp}^2g_{\|}^2(140.50)+g_{\|}^4(0.50)]. \tag{2}$$

In this formula a is the cubic unit cell edge, $g_{\|}$ and $g_{\perp}$ are the diagonal elements of the axially symmetric g tensor, and $P=(g_{\|}^2+2g_{\perp}^2)/3$. The small size of the final term in this expression is due to the peculiar structure of the KY_3F_{10} materials, and indicates that θ_W^{dip} by itself is not a good indicator of the strength of dipolar interactions when the moment is Ising-like. θ_W^{dip} also vanishes, as expected from the cubic symmetry, when the moment is isotropic. The value of $g_{\|}$ in KEr_3F_{10} is nearly 18, the maximum possible for a doublet state in Er^{3+}, indicating that the ground state consists almost entirely of $|J=\frac{15}{2},J_z=\pm\frac{15}{2}\rangle$, for which $g_{\|}=18$ and $g_{\perp}=0$. This is predicted as well by the crystal field analysis. The experimental g factors predict $\theta_W^{dip}=0.047$ K, so $\theta_W^{ex}=\theta_W-\theta_W^{dip}=-0.76\pm0.15$ K and exchange is antiferromagnetic in this material.

Figure 4 shows the inverse susceptibility from 0 to 2.5 K of KYb_3F_{10}. This material remains paramagnetic to much lower temperatures, with the susceptibility reaching a maximum of 7.97 cm^3/mol in the vicinity of 10 mK, and remaining roughly constant below that temperature. The maximum value of the dimensionless susceptibility is 0.214, about 90% of the demagnetization limit for a sphere, strongly suggesting a spontaneous magnetization. The ZFC susceptibilities below ~20 mK are again substantially smaller. The susceptibility

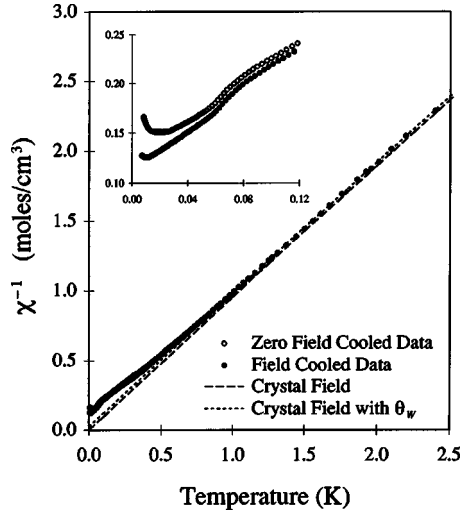

FIG. 4. Inverse susceptibility of KYb_3F_{10} below 2.5 K. The FC susceptibility becomes roughly temperature independent below approximately 10 mK, with a magnitude equal to 90% of the demagnetization limit, strongly suggesting ferromagnetism. The inset shows the full range of zero-field-cooled data at lower temperatures. From 1 to 2.5 K, the susceptibility follows a Curie-Weiss law.

follows a Curie-Weiss law accurately from 1 to 2.5 K, yielding $\theta_W=-0.022\pm0.009$ K and a Curie constant $C=1.07\pm0.1$ cm^3 K/mol. Two measurements of the g factors of Yb^{3+} in the KY_3F_{10} structure have been reported: $g_{\|}=5.383$, $g_{\perp}=1.310$,[13,17,18] and $g_{\|}=5.363$, $g_{\perp}=1.306$.[19] These values are consistent only with a Yb^{3+} ground doublet which is approximately $0.98|J=\frac{7}{2},J_z=\pm\frac{5}{2}\rangle+0.2|J=\frac{7}{2},J_z=\mp\frac{3}{2}\rangle$. Both sets of values yield $\theta_W^{dip}=0.068$ K, leading to $\theta_W^{ex}=-0.090\pm0.009$ K, again implying antiferromagnetic exchange. The Curie constant for the ground doublet of Yb^{3+} in this structure is calculated to be $C^{calc}=1.013$ cm^3 K/mol using the data of Ref. 18, and 1.006 cm^3 K/mol using that of Ref. 19, both in reasonably close agreement with the experimental value.

The inverse susceptibility of the third compound, KTm_3F_{10}, is pictured in Fig. 5 from 0 to 2.0 K. It exhibits a sharp, cusplike minimum in the vicinity of 0.2 K, and rises sharply below that temperature. Between approximately 0.1 K and 10 mK the susceptibility levels off at a value of roughly 35% of its maximum at the cusp; below 10 mK it continues to decrease. FC and ZFC susceptibilities agree below the temperature of the cusp down to about 150 mK, but below that temperature the ZFC values are substantially smaller. The cusp near 0.2 K is most consistent with an antiferromagnetic ordering feature, although the maximum in the dimensionless susceptibility is equal to 0.13, about 55% of the demagnetization limit for the sample. The plateau in susceptibility below 0.1 K, coupled with the divergence of FC and ZFC data, may indicate a second phase transition, perhaps to a disordered state, or alternatively a ferromagnetic state with substantial pinning of the domain walls. The value of $\chi_{\max}$ was reproducible to 8% between two different samples, but the value of the plateau in χ was less reproducible, lying 30% lower in the second sample (not shown).

From 7 K to 20 K, the susceptibility of KTm_3F_{10} follows a Curie-Weiss behavior accurately, shown in Fig. 6, yielding

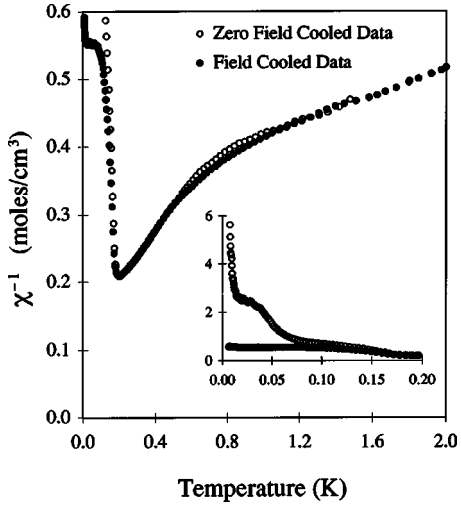

FIG. 5. Inverse susceptibility of KTm_3F_{10} below 2.0 K. This material has Ising-like moments like KEr_3F_{10} and KYb_3F_{10}, but shows a sharp cusp in the vicinity of 0.2 K. Both FC and ZFC susceptibilities decline rapidly below this point, diverging only at temperatures below 0.15 K. The inset shows the full range of ZFC data below 0.2 K.

$\theta_W = -0.64 \pm 0.15$ K and a Curie constant $C = 6.29 \pm 0.5$ cm^3 K/mol. The g factors of this material have not been directly measured. Optical spectroscopy[20] reveals the lowest Stark sublevels for Tm^{3+} in this structure to be two nearly degenerate singlets, separated by less than 1 K. From the derived crystal-field parameters, one is a nearly pure antisymmetric singlet of the form $|J=6, J_z=+6\rangle - |J=6, J_z=-6\rangle$. The other is a nearly pure symmetric conjugate $|J=6, J_z=+6\rangle + |J=6, J_z=-6\rangle$. The next excited state lies almost 500 K higher. Because of the very small splitting between the two singlets, they behave as an effective doublet $|J=6, J_z=\pm 6\rangle$ down to temperatures of order 1 K, with predicted g factors of $g_\parallel = 14$ and $g_\perp = 0$. The Curie constant

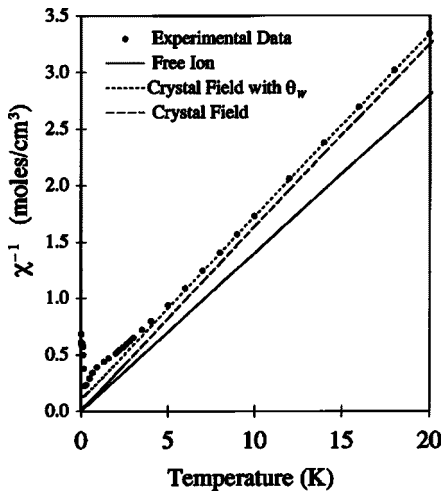

FIG. 6. Inverse susceptibility of KTm_3F_{10} from 0 to 20 K, with a mean-field fit to data above 7 K, where a Curie-Weiss law is obeyed. The lower dashed curve is the calculated inverse susceptibility without interactions, χ_o^{-1}. The upper dashed curve denotes $\chi_o^{-1} - \lambda$, where $\lambda = \theta_W / C$ is the fitted mean field parameter.

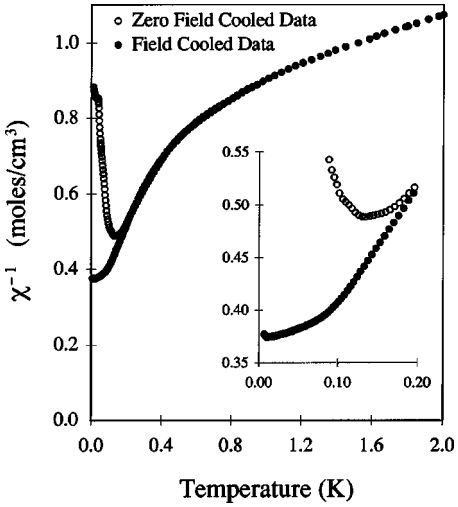

FIG. 7. Inverse susceptibility of KTb_3F_{10} below 2 K. The susceptibility reveals a magnetic ground state for the Tb^{3+} ion in this structure, with a relatively small moment below 0.6 K. While qualitatively similar to the behavior of KEr_3F_{10} and KYb_3F_{10}, the maximum dimensionless susceptibility is only 29% of the demagnetization limit here. The inset shows an expansion of the region below 0.2 K.

predicted by these values is $C^{calc} = 6.13$ cm^3 K/mol, within 3% of the experimental value. This agreement strongly suggests that KTm_3F_{10} also has Ising-like moments. Equation (2) predicts $\theta_W^{dip} = 0.010$ K for KTm_3F_{10}, leading to an antiferromagnetic $\theta_W^{ex} = -0.65 \pm 0.15$ K.

Figure 7 shows the inverse susceptibility of KTb_3F_{10} below 2 K. It exhibits paramagnetic behavior down to temperatures below 0.2 K, whereupon field-cooled and zero-field-cooled data begin to diverge strongly. The FC susceptibility shows a kink in the vicinity of 80 mK, below which it increases more slowly. The susceptibility begins to drop below a second kink in the vicinity of 10 mK. It is possible that KTb_3F_{10} orders with a spontaneous magnetization, so that the divergence between FC and ZFC data reflects increased pinning of domain wall boundaries at temperatures below T_c. In its qualitative features, the susceptibility of KTb_3F_{10} certainly resembles the ferromagnetic behavior of the related Dy, Er, and Yb compounds more than that of KTm_3F_{10}. However, for KTb_3F_{10} the maximum dimensionless susceptibility is equal to 0.069, slightly less than 30% of the demagnetization limit $N^{-1} = (4\pi/3)^{-1} = 0.239$ for a spherical sample. Alternatively, the history dependence in the susceptibility could possibly indicate a disordered or spin-glass ground state.

There are no published crystal-field parameters directly measured in KTb_3F_{10}, and so we do not know the ground state of the Tb^{3+} ion with certainty. Interpolating the parameters of neighboring lanthanide ions in the KY_3F_{10} structure[12,13] predicts a ground state which is a nearly pure singlet $|J=6, J_z=0\rangle$. The next higher state is a non-Kramers doublet approximately 20 cm^{-1} above which is principally $|J=6, J_z=\pm 1\rangle$, with small admixtures of $|J=6, J_z=\pm 5\rangle$ and $|J=6, J_z=\mp 3\rangle$. Theoretically calculated crystal-field parameters lead to a similar conclusion.[21] This prediction conflicts with the experimental susceptibility, which shows a magnetic

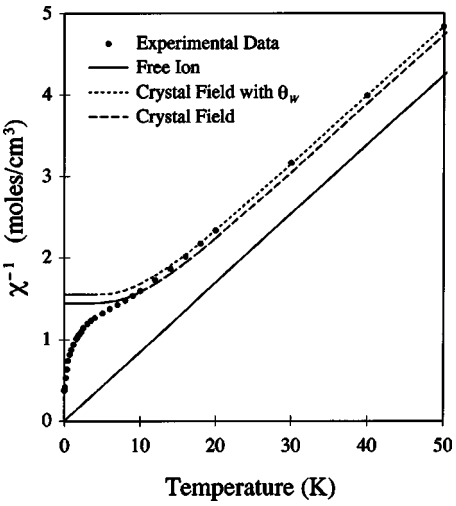

FIG. 8. Inverse susceptibility of KTb_3F_{10} from 0 to 50 K, with a mean-field fit to data above 30 K. Crystal field parameters extrapolated from other members of this series (Refs. 12 and 13), as well as theoretical estimates (Ref. 21), fail to predict the magnetic ground state of Tb^{3+} in KTb_3F_{10}, but fit the susceptibility accurately above 30 K.

ground state for Tb^{3+} with a rather small moment below about 0.6 K. The hyperfine interaction in Tb^{3+} is at least two orders of magnitude too small to account for this. An impurity moment cannot explain it either; the magnitude of the low temperature susceptibility would require at least a 10% Er impurity, which is an order of magnitude above the maximum inferred from the high-temperature Curie constant. Even more is required if the impurity is any other rare earth. The data are most consistent with an inverted arrangement of the bottom two states in which the doublet lies lowest. In this case the Tb^{3+} moment, as a non-Kramers doublet, would be Ising-like, with $g_\perp = 0$.

Figure 8 shows a mean-field fit to the susceptibility data above 30 K, where the result is insensitive to the arrangement of the lowest-lying states, using the extrapolated crystal field parameters. This procedure yields a mean-field interaction parameter $\lambda = -0.12 \pm 0.02$ mol/cm^3. Then $\theta_W = C\lambda < 0$, and $|\theta_W| > 0.034 \pm 0.006$ K, using the minimum possible Curie constant for Tb^{3+}, corresponding to a ground state $|J=6, J_z = \pm 1\rangle$. From this, $\theta_W^{ex} = \theta_W - \theta_W^{dip} = ([g_\parallel \mu_B]^2/4k_B) \times (N_0\lambda/3 - 1.5/a^3) \cong \theta_W$, so exchange is antiferromagnetic in this material as well.

It is possible that the symmetry of the Tb^{3+} crystalline environment at low temperature may be different from the other members of this series of compounds. KTb_3F_{10} lies at the low-mass limit of stability of the KLn_3F_{10} series (KGd_3F_{10} does not form with this structure, although $RbGd_3F_{10}$ does[22]), and a crystalline distortion to lower symmetry at low temperature cannot be ruled out, although a conventional Jahn-Teller instability would not leave a doublet lying lowest.

To interpret these results we performed a numerical energy minimization calculation of the magnetic Hamiltonian at $T=0$, following the procedure of Ref. 7. Assuming isotropic exchange, the Hamiltonian is[23,24]

$$\mathrm{H} = \frac{1}{2}\sum_{ij}\frac{1}{r_{ij}^3}\left[\vec{\mu}_i \cdot \vec{\mu}_j - 3\frac{(\vec{\mu}_i \cdot \vec{r}_{ij})(\vec{\mu}_j \cdot \vec{r}_{ij})}{r_{ij}^2}\right] - \sum_{ij} J_{ex}\vec{S}_i \cdot \vec{S}_j - D\sum_i S_{i\parallel}^2, \tag{3}$$

where $\vec{\mu}_i = \mu_B[\mathbf{g}_i]\vec{S}_i$, $[\mathbf{g}_i]$ is the local g tensor for spin i,[25,26] and nearest neighbor exchange is assumed, but the dipolar interaction is long ranged. D is a single-ion anisotropy coefficient and $S_{i\parallel}$ denotes the component of $\vec{S}_i$ parallel to the local tetragonal symmetry axis. A rough estimate of D can be obtained from the splitting δ between the ion's ground state and first excited state in these materials. At temperatures of order δ and above, the calculated single-ion susceptibility is much less anisotropic, implying an effective anisotropy constant $D \sim \delta$. Spectroscopically determined splittings for Er, Yb, and Tm (Refs. 13 and 20) are listed in Table I, with a value for Tb estimated from extrapolated crystal field parameters. They range from the rather suspect value of 34 K for Tb^{3+} to nearly 500 K for Tm^{3+}. The exchange constant is obtained from $\theta_W^{ex} = 2zS(S+1)J_{ex}/3k_B$, where the number of nearest neighbors z for this structure is taken to be 8 and the effective spin S of the ground doublet of each rare-earth ion is 1/2. The derived values of J_{ex}/k_B are listed in Table I for the Er, Yb, and Tm compounds; they are all less than 1 K in magnitude. The single ion anisotropy term in the Hamiltonian is therefore large compared to the interaction terms, and the spins (assumed Heisenberg-like in the beginning) will be nearly aligned with their local symmetry axes. If we

TABLE I. Experimental values of the Stark splitting δ between the magnetic ion's ground and first excited states, mean-field interaction constant λ, Weiss constant, calculated minimum dipole-dipole interaction energies per spin ε_d, and various derived quantities for four compounds having KY_3F_{10} structure and Ising-like moments.

	δ (K)	λ (mol/cm^3)	θ_W (K)	J_{ex}/k_B (K)	ε_d/k_B (K)	J_{ex}/ε_d
KEr_3F_{10}	71[a]	-0.070 ± 0.015	-0.71 ± 0.15	-0.19 ± 0.04	-1.45	0.13
KYb_3F_{10}	196[b]	-0.025 ± 0.008	-0.022 ± 0.009	-0.023 ± 0.002	-0.14	0.16
KTm_3F_{10}	490[c]	-0.100 ± 0.015	-0.64 ± 0.15	-0.16 ± 0.04	-0.935	0.17
KTb_3F_{10}	34?	-0.12 ± 0.02	$< -0.034 \pm 0.006$	$< -0.008 \pm 0.002$		0.21

[a]Reference 11.
[b]Reference 13.
[c]Reference 20.

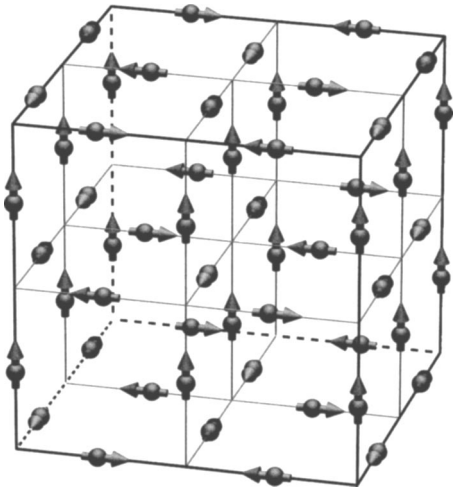

FIG. 9. Dipolar ferromagnetic state lying slightly above the antiferromagnetic ground state, obtained by minimizing the Hamiltonian of Eq. (3) with $J_{ex}=0$. Only the magnetic spins within the cubic unit cell are shown. The AF dipolar ground state differs from that pictured only in having the vertical chains of spins alternate up and down; the small splitting between the two states, per spin, is $\Delta=1.6(g_{\|}\mu_B S)^2/a^3$.

assume the alignment is complete, so that the spins are perfectly Isinglike, the exchange term will be identically zero, since nearest-neighbor spins are all orthogonal.

If exchange is therefore initially ignored, minimization of the Hamiltonian at $T=0$ predicts a purely dipolar ground state which is Ising-like and antiferromagnetic, with energy per spin of approximately $\varepsilon_d=-46.0(g_{\|}\mu_B S)^2/a^3$. This disagrees with the experimental results for the Er and Yb compounds, similar to our earlier findings for KDy_3F_{10}, and indicates that the dipolar interaction alone cannot generally predict the ordered state in the KY_3F_{10} compounds, unlike the $LiYF_4$ materials.

In the absence of exchange, a ferromagnetic energy minimum lies slightly above the antiferromagnetic ground state described above, split by an energy per spin given approximately by $\Delta=1.6(g_{\|}\mu_B S)^2/a^3$. This spin arrangement is pictured in Fig. 9. The AF ground state differs only in that the head-to-tail chains along the vertical z axis alternate up and down. For the Er, Yb, and Tm compounds, the dipolar energy ε_d is roughly 5–7 times J_{ex} in magnitude, indicating that while the dipolar interaction is larger, exchange is not negligible. When AF exchange is included, the theoretical model of Ref. 7 predicts that the alternating spins lying in the x-y plane of Fig. 9 rotate slightly downward, so that, surprisingly, the energies of the FM and AF states cross for sufficiently large J_{ex}. The ferromagnetic state lies lowest for J_{ex} exceeding

$$J_{ex}^{crit} \cong -2\left(\left[\frac{2}{3}D - Q_d\right]\Delta\right)^{1/2}/n_1 S, \tag{4}$$

where Q_d is a dipolar energy sum given approximately by $-38.56(g_{\|}\mu_B)^2/a^3$. n_1 is the average number of $S_z-S_{x,y}$ nearest neighbor pairs, per spin. For the predicted ferromagnetic state, $n_1=16/3$.

In the case of KDy_3F_{10} reported earlier,[7] the exchange and dipolar interactions are comparable in magnitude, and D is no more than 10 K, so that the magnitude of J_{ex} exceeds the estimate above and ferromagnetism is both predicted and observed. For the Er, Yb, and Tm compounds, exchange is relatively weaker in comparison to the dipolar interaction, as shown in Table I, and D is larger. For all three, J_{ex} is roughly an order of magnitude smaller than J_{ex}^{crit} obtained from Eq. (4), the value necessary to stabilize ferromagnetism. Despite these differences, the experimental behavior of KEr_3F_{10} and KYb_3F_{10} is essentially similar to that of KDy_3F_{10}. The discrepancy between calculation and experiment may possibly be due to an overestimate of the strength of the single-ion anisotropy by the relation $D\sim\delta$. There is also an appreciable likelihood that exchange is not isotropic, including the possibility that J_{ex} is underestimated by the relation $\theta_W^{ex}=2zS(S+1)J_{ex}/3k_B$.

Equation (4) predicts that ferromagnetism is less favorable as the anisotropy constant D increases, for a given J_{ex}. In agreement with this, it is noteworthy that only the Tm compound displays a cusplike ordering feature characteristic of antiferromagnetism, and this material has by far the largest value of D. In other words, KTm_3F_{10} is the most rigidly Ising-like of these materials, so its spins cannot rotate enough for a ferromagnetic ground state to lie lowest. Using either the critical or the experimental values of J_{ex}, we calculate the transverse component of S to be $S_\perp/S\cong -J_{ex}n_1/2\left(\frac{2}{3}D-Q_d\right)<0.1$ in all four materials, so the predicted deviation from Ising-like symmetry is small, and the overall spin-spin interaction energy is predominantly dipolar in origin. This is a consequence of the peculiar structure of the KY_3F_{10} materials, wherein the large single-ion anisotropy constrains exchange to be artificially small compared to the dipolar energy.

IV. CONCLUSIONS

In conclusion, we have measured the magnetic properties of KEr_3F_{10}, KYb_3F_{10}, KTm_3F_{10}, and KTb_3F_{10}, cubic systems with axial moments nearly aligned along the three mutually orthogonal cubic axes. For all four compounds, susceptibility measurements indicate that exchange is antiferromagnetic, and calculation shows that the dipole-dipole interaction alone also favors antiferromagnetism. Despite this, we find that only the Tm compound clearly shows antiferromagnetic behavior, while the Er and Yb compounds order ferromagnetically. By numerically minimizing the Hamiltonian at $T=0$, we find that these results can be understood in terms of the strength of the exchange constant: the magnitude of J_{ex} must exceed a critical value, dependent on single-ion anisotropy and the dipole-dipole interaction strength, for ferromagnetism to occur.

ACKNOWLEDGMENT

We acknowledge helpful discussions of these results with R.R.P. Singh.

*Present address: Boxer Cross, Inc., Menlo Park, CA 94025.
†Email address: corruccini@physics.ucdavis.edu

[1] J. W. Pierce and Y.-P. Hong, in *Proceedings of the Tenth Rare Earth Research Conference*, Carefree, Arizona, 1973, edited by Clement J. Kevane and Therald Moeller (U.S. Atomic Energy Commission, Technical Information Center, Oak Ridge, TN, 1973), p. 529; distributed by National Technical Information Service, Springfield, VA.
[2] D. Bitko, T. F. Rosenbaum, and G. Aeppli, Phys. Rev. Lett. **77**, 940 (1996), and references therein.
[3] G. Mennenga, L. J. de Jongh, and W. J. Huiskamp, J. Magn. Magn. Mater. **44**, 59 (1984).
[4] S. K. Misra and J. Felsteiner, Phys. Rev. B **15**, 4309 (1977).
[5] P. Beauvillain, J.-P. Renard, and P.-E. Hansen, J. Phys. C **10**, L709 (1977).
[6] S. T. Bramwell and M. J. P. Gingras, Science **294**, 1495 (2001).
[7] S. L. Chamberlain, G. Luo, and L. R. Corruccini, Phys. Rev. B **67**, 134414 (2003).
[8] S. Aleonard, J. C. Guitel, and M. T. Roux, J. Solid State Chem. **24**, 331 (1978).
[9] M. Labeau, S. Aleonard, A. Vedrine, R. Boutonnet, and J. C. Cousseins, Mater. Res. Bull. **9**, 615 (1974).
[10] M. J. Weber, R. Morgret, S. Y. Leung, J. A. Griffin, D. Gabbe, and A. Linz, J. Appl. Phys. **49**, 3464 (1978).
[11] E. Antic-Fidancev, M. Lemaitre-Blaise, and P. Porcher, Proceedings of the International Symposium of Rare-Earth Spectroscopy, Wroclaw, Poland, 1984, edited by B. Jezowska-Trzebiatowska, J. Legendziewicz, and W. Strek (World Scientific Singapore, Philadelphia, 1985), p. 134.
[12] A. V. Vinokurov, R. S. Zhdanov, A. L. Stolov, and S. I. Yagudin, Phys. Solid State **38**, 415 (1996).
[13] R. Yu. Abdulsabirov, A. V. Vinokurov, V. A. Ivanshin, I. N. Kurkin, E. A. Pudovik, A. L. Stolov, and Sh. I. Yagudin, Opt. Spectrosc. **63**, 55 (1987).
[14] M. R. Roser and L. R. Corruccini, Phys. Rev. Lett. **65**, 1064 (1990).
[15] A. H. Cooke, D. A. Jones, J. F. A. Silva, and M. R. Wells, J. Phys. C **8**, 4083 (1975).
[16] J. M. Daniels, Proc. Phys. Soc., London, Sect. A **66**, 673 (1953).
[17] R. Yu. Abdulsabirov *et al.*, Sov. Phys. Crystallogr. **32**, 559 (1987).
[18] V. A. Ivanshin, I. N. Kurkin, I. Kh. Salikhov, and Sh. I. Yagudin, Sov. Phys. Solid State **28**, 1448 (1986).
[19] M. Yamaga, M. Honda, J.-P. R. Wells, T. P. J. Han, and H. G. Gallagher, J. Phys.: Condens. Matter **12**, 8727 (2000).
[20] M. Diaf, A. Braud, C. Labbe, J. L. Doualan, S. Girard, J. Margerie, R. Moncorge, and M. Thuau, Can. J. Phys. **77**, 693 (1999).
[21] C. A. Morrison, D. F. Wortman, R. P. Leavitt, and H. P. Jenssen, Report HDL-TR-1897, Harry Diamond Laboratory, Adelphi, MD 20783, USA, 1980.
[22] S. L. Chamberlain and L. R. Corruccini, J. Magn. Magn. Mater. **264**, 158 (2003).
[23] R. Moessner, Phys. Rev. B **57**, R5587 (1998).
[24] T. Niemeijer and P. H. E. Meijer, Phys. Rev. B **10**, 2962 (1974).
[25] A. Abragam and B. Bleaney, *Electron Paramagnetic Resonance of Transition Ions* (Oxford University Press, London, 1970), p. 13.
[26] M. Marrenga and T. Niemeijer, Physica (Amsterdam) **78**, 469 (1974).